Earth and Planetary Science Letters 312 (2011) 48–58

Contents lists available at SciVerse ScienceDirect

Earth and Planetary Science Letters

journal homepage: www.elsevier.com/locate/epsl

The role of fluid residence time and topographic scales in determining chemical fluxes from landscapes

K. Maher

Department of Geological and Environmental Sciences, Braun Hall #118, 450 Serra Mall, Stanford University, Stanford, CA 94305, United States

ARTICLE INFO

Article history:
Received 26 April 2011
Received in revised form 20 September 2011
Accepted 25 September 2011
Available online 28 October 2011

Editor: G. Henderson

Keywords:
chemical weathering
solute fluxes
global carbon cycle
erosion
climate change

ABSTRACT

The role of fluid residence time and catchment length scales in controlling the chemical composition of rivers is evaluated by comparing numerical simulations and scaling arguments to concentration–discharge data from small catchments. The analysis suggests that poorly-crystalline aluminosilicates are an important control on the composition of stream waters and therefore chemical equilibrium between the dissolving and precipitating phases determines the maximum concentration and the maximum silicate weathering flux. The modeling results suggest that the residence time of fluid relative to the residence time required to approach chemical equilibrium can be used to assess the controls on solute fluxes in small catchments, and possibly larger rivers. Catchments that show little variability in concentration with discharge (or "chemostatic behavior") likely have average fluid residence times that exceed the time required to reach chemical equilibrium. Conversely, decreases in concentration with increasing discharge are explained by average residence times shorter than required to approach chemical equilibrium, resulting in dilution. Solute fluxes are also strongly impacted by the distribution of fluid residence times in a basin. The fluid residence time model provides an alternative framework for assessing both the relationship between discharge and concentration observed for individual catchments, and controls on the solute fluxes of rivers. If fluid residence times are a dominant control on weathering fluxes, the chemistry of different rivers could vary entirely as a function of the nature subsurface flow paths and the composition of the system at equilibrium, which is complex to predict and strongly coupled to biological processes, temperature and the composition of the system. As a result of thermodynamic and hydrologic restrictions on the amount of weathering, global solute fluxes may depend more strongly on the geometry, relief, runoff and permeability of basins then on temperature and rates of erosion.

1. Introduction

The flux of dissolved silicate and carbonate rock is an important control on the composition of the oceans and the atmosphere. In most treatments of global elemental cycles, weathering fluxes in the past are scaled according to semi-empirical formulations that account for runoff, temperature, erosion and biological processes (Arvidson et al., 2006; Berner and Kothavala, 2001; Wallmann, 2001). These scaling parameters are often based on observations from modern rivers of varying sizes and climates, and are thus assumed to apply in the past (Dessert et al., 2003; Gaillardet et al., 1999; Ludwig et al., 1998). An alternative approach to modeling solute fluxes is to develop a mechanistic but simple model for solute production and test it against modern river chemistry. Such a model must incorporate the effects of runoff, erosion, temperature and biological processes, while avoiding the incorporation of empirical parameters that may have varied in the past. Such a model must also consider how fluids travel through the zone of solute generation and the thermodynamic constraints that limit solute generation.

The ability to accurately predict the generation of solutes is integral to understanding the relationships between climate, tectonic uplift/erosion and chemical weathering (West et al., 2005). In many catchments, solute fluxes are linearly correlated with discharge, suggesting that solute concentrations are constant over a broad range of discharge (Godsey et al., 2009; Stefansson and Gislason, 2001). Even for large rivers draining diverse lithologies, a nearly linear relationship is observed between solute flux and discharge (Gaillardet et al., 1999). This behavior has been called "chemostatic" and has been interpreted as evidence for strong climatic or hydrologic control of solute fluxes (Clow and Mast, 2010; Godsey et al., 2009).

Models of the relationship between concentration and discharge are also commonly used in catchment hydrology. Physical models often relate concentration–discharge relationships to mixing of end-member waters from different physical locations in the landscape (Evans and Davies, 1998). Chemical models can be differentiated into several categories: models that assume fluxes depend on reaction rates (Godsey et al., 2009), models that assume the concentration

E-mail address: kmaher@stanford.edu.

0012-821X/$ – see front matter © 2011 Elsevier B.V. All rights reserved.
doi:10.1016/j.epsl.2011.09.040

varies as a function of the subsurface contact time (Anderson et al., 1997a; Hornberger et al., 2001; Johnson et al., 1969), and models that assume solute concentrations are determined by chemical equilibrium between a primary and secondary phase (Bowser and Jones, 2002; Drever and Zobrist, 1992; Garrels and Mackenzie, 1967; Stefansson and Gislason, 2001; Tardy, 1971). Models that neglect chemical equilibrium would allow for concentrations to surpass equilibrium values, whereas models that assume chemical equilibrium would not predict lower concentrations when fluids are not chemically equilibrated, especially at high discharge or short subsurface contact times. Thus, any model linking solute fluxes to physical or chemical processes must consider both kinetic and equilibrium processes.

The goal of this work is to develop a conceptual framework for solute generation in catchments that can explain the response of rivers to changes in observable parameters such as discharge, temperature and the residence time of fluids in the subsurface. This conceptual framework must take into account the balance between chemical equilibrium, kinetic and hydrologic controls. To accomplish this, a numerical model is used to assess the extent of chemical equilibration along a flow path for different parameters known to impact solute generation (e.g. mineral composition, temperature, soil gas CO_2 concentration, water content, flow rate and effective surface area). The numerical model results are used to develop a scaling approach that can describe chemical fluxes as a function of the ratio of the actual fluid residence time to the time required to reach chemical equilibrium. The model is then tested against concentration–discharge data from single rivers. If it can be shown to scale with catchment size, this framework provides an alternative approach for interpreting solute fluxes from catchments that can be used to evaluate rates of chemical denudation or concentration–discharge relationships.

2. Methods

2.1. Conceptual model

The residence time of water is expected to be an important control on solute concentrations because longer transit times favor the accumulation of more solute (Berner, 1978; Wolock et al., 1997). Tracer studies of small headwater catchments yield mean residence times of water ranging from a few months to several years (Asano et al., 2002; McGuire and McDonnell, 2006, 2010; McGuire et al., 2002; McGuire et al., 2005; McGuire et al., 2007; Soulsby et al., 2000; Stewart et al., 2010; Tetzlaff et al., 2009). For large river basins, mean residence times can approach decades because of longer flow paths (McGuire and McDonnell, 2006). Fig. 1 depicts the possible flow paths through the hillslope to the stream and the chemical evolution along the flow path. The hydrologic setting is simplified to focus on the chemical aspects of solute generation and to highlight the importance of the ratio between the flow path length (L) and the flow path length required to reach chemical equilibrium (L_{eq}), where the later can depend on a number of different factors including water flux, water content, mineral surface area, soil gas PCO_2 and the equilibrium concentration (Maher, 2010). This conceptual model emphasizes the importance of physical length scales relative to chemical length scales as an important factor in solute fluxes.

2.2. Data sources

Runoff generation is clearly a dynamic process so it is surprising that many catchments show minimal variation in solute concentrations across wide ranges of discharge. To assess model predictions

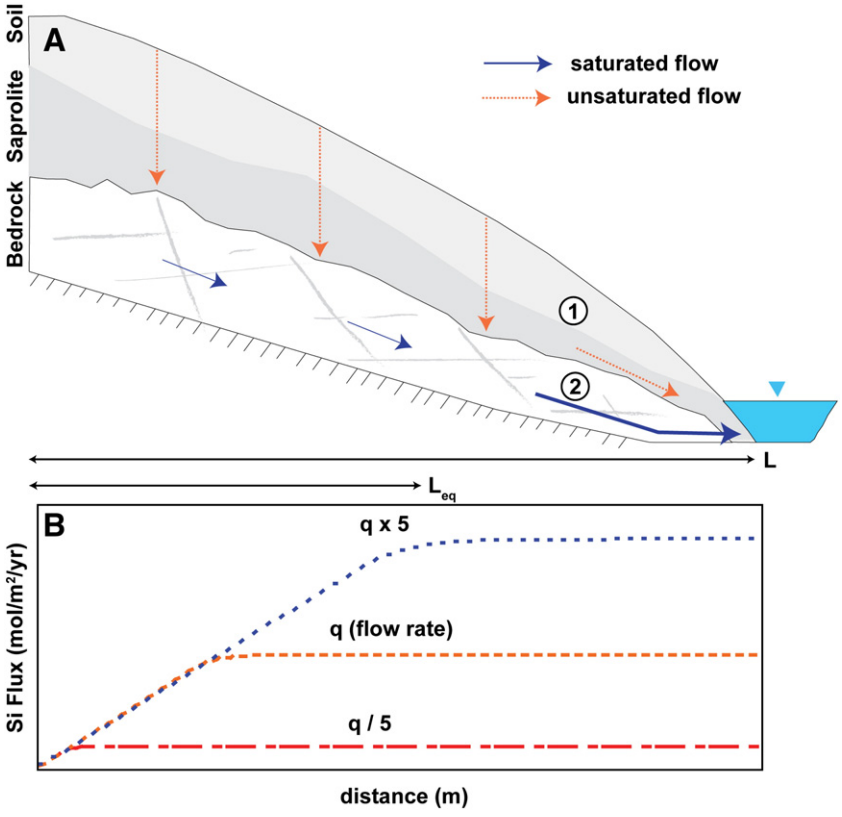

Fig. 1. Conceptual model for the generation of solute fluxes due to gradual equilibrium along a flow path. (A) Schematic of subsurface flow paths showing the paths that water may follow to the channel depending on the soil–bedrock boundary and the seasonal moisture distribution (modified from Anderson et al., 1997b; McDonnell et al., 2010). Seasonal preferential flow (not shown) may also be important. The pathways of (1) shallow unsaturated flow and (2) deep groundwater represent two important zones of solute generation. (B) Schematic of the increase in solute flux with distance along the flow path as a function of different flow rates. The maximum solute flux is achieved when equilibrium is reached between the primary dissolving feldspars and the secondary aluminosilicate. The relevant length scales are depicted by L, the length of the flowpath, and L_{eq}, the distance where the fluid reaches equilibrium (L_{eq} is shown for the high flux case ($q \times 5$)).

of concentration and discharge, sites from the United States Geological Survey's (USGS) Hydrologic Benchmark Network (HBN) (http://ny.cf.er.usgs.gov/hbn/index.cfm) are used (Mast and Clow, 2000). The mean annual discharge–weighted concentrations (calculated following Godsey et al., 2009; Zeman, 1978) show the same general trends as the individual events so the individual events are used for the model fitting and evaluation. The data were not corrected for rainfall inputs or evapotranspiration in order to accurately compute mineral saturation states. Fig. 2A shows Si flux as a function of runoff illustrating the approximate "chemostatic" behavior for individual catchments as noted by Godsey et al. (2009). Fig. 2B shows the concentration–discharge relationships for three catchments indicating the three general patterns observed: (1) decreasing concentration with increasing discharge, (2) constant concentration or "chemostatic" behavior and (3) decreasing concentration only at high discharge.

2.3. Reactive transport simulations

The reactive transport code CrunchFlow (Maher et al., 2006; Maher et al., 2009; Steefel, 2001; Steefel and Maher, 2009) was used to evaluate the increase in solute concentrations as a function of flow rate, temperature, mineral surface areas, water saturation and soil gas CO_2 (PCO_2). The model simulations were run at 5 °C, 15 °C and 25 °C and 1 atm, with 15 °C representing the average global temperature (Berner and Kothavala, 2001). The model domain consisted of a one dimensional soil column with a flux boundary condition at the base of the profile, and a Dirichlet boundary condition for aqueous and gaseous species at the land–atmosphere interface. The simulations infiltrated dilute rainwater into a variably water saturated column of minerals with a porosity of 17.5%. The simulations were run with a starting composition approximating granite (18.2 wt.% plagioclase (20% anorthite (An_{20})), 18.2 wt.% K-feldspar, 60.6 wt.% quartz, and 3 wt.% secondary minerals). Mineral surface areas were 0.5 m^2/g for feldspars and 10 m^2/g for secondary minerals corresponding to the ranges of values for feldspars reported in White and Brantley (2003) and for clay minerals (Maher et al., 2009; Yang and Steefel, 2008).

The majority of the equilibrium constants for minerals and the relevant aqueous complexes used in the modeling and interpretation are from the EQ3/EQ6 thermodynamic database (Wolery et al., 1990). Log K values for anorthite/albite solid solution series are from Arnorsson and Stefansson (1999). The rate constants and activation energies are from a compilation by Palandri and Kharaka (2004). The kinetic rate law for feldspar dissolution includes a non-linear dependence on Al activity and feldspar saturation state (Gautier et al., 1994; Maher et al., 2006; Maher et al., 2009; Oelkers et al., 1994; Schott et al., 2009). Model profiles shown in Fig. 1B (and subsequently) correspond to 500 years, ample time to reach quasi-steady state such that the fluid compositions are not changing appreciably over time at a given point (Lichtner et al., 1986).

In a multi-component system characterized by irreversible reactions, the reaction endpoint is highly dependent on the mineral kinetics and the components in the system (Lasaga et al., 1994; Steefel and Van Cappellen, 1990). The goal of this study is to understand how departures from chemical equilibrium affect solute fluxes, and not to determine the exact phases that control the equilibrium concentrations as these may vary with climate, vegetations and lithology. Fig. 3 shows the water compositions for the majority of the HBN catchments are also consistent with either kaolinite or a metastable aluminosilicate (likely halloysite). Saturation with respect to halloysite, allophane or imogolite is common for both river waters (Stefansson and Gislason, 2001) and soil waters (Maher et al., 2009; White et al., 2009). As a result, the model mineral system that produced the most consistent values for pH, Si, K, Na compared to the HBN river data was composed of quartz, K-feldspar, plagioclase (An_0 to An_{20}) and halloysite (Fig. 3). The dashed lines in Fig. 3 show that the phase boundaries will shift depending on the solubility of the secondary aluminosilicate, and in general the identity and solubility of the secondary minerals are poorly known (Violette et al., 2010; Yang and Steefel, 2008). However, clay minerals composed of the more soluble elements (such as smectite) tend to form in dry environments, while kaolinite group minerals tend to form in wetter climates (Chadwick and Chorover, 2001; Curtis, 1990; Folkoff and Meentemeyer, 1985). Most of the basins considered have rainfall amounts typical of halloysite, consistent with the model predictions. Overall the chemical endpoints in the model are highly uncertain, yet the overall progression towards chemical equilibrium is not.

3. Results

3.1. Reactive transport model sensitivity analysis

Reactive transport simulations were used to evaluate the sensitivity of solute profiles to key variables (Fig. 4). The goal is to understand: (1) the parameters that impact the final equilibrium concentration and (2) the parameters that control the time required for fluids to equilibrate. The equilibrium time and concentration relative to the system length scale determine the maximum solute flux and are thus important

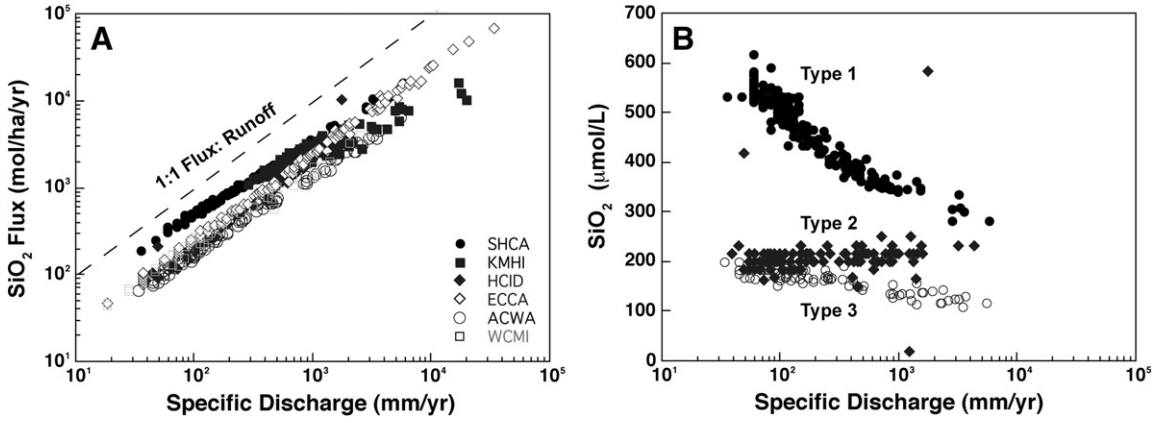

Fig. 2. (A) Silica flux as a function of specific discharge for the United States Geological Survey's (USGS) Hydrologic Benchmark Network (HBN) sites described in Mast and Clow (2000). Some sites were also considered by Godsey et al. (2009). Each type of symbol represents a different catchment from HBN (SHCA, Sagehen, CA; KMHI, Kahakuloa Stream, HI; HCID, Hayden Creek, ID; ECCA, Elder Creek, CA; ACWA, Andrews Creek, WA; Washington Creek, MI). Data plotted are individual discharge concentrations measurements. Dashed line represents a 1:1 relationship between solute fluxes and runoff indicative of constant concentration. (B) HBN data for SiO_2(aq) concentration as a function of specific discharge showing the three types of commonly observed concentration–discharge relationships: (1) complex dilution, (2) constant concentration and (3) constant concentration until a threshold in discharge is exceeded.

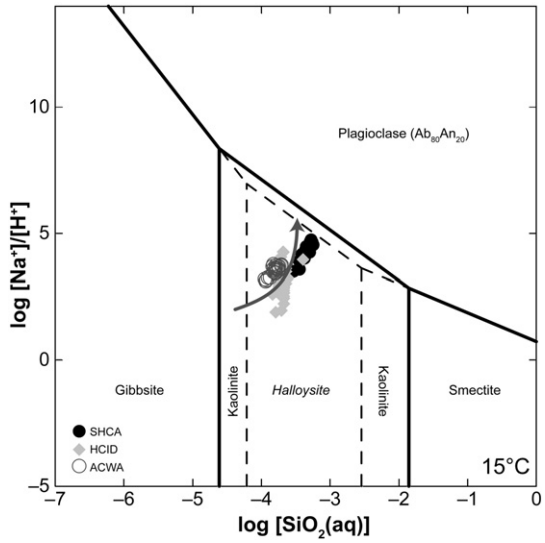

Fig. 3. Activity diagram for plagioclase, gibbsite, smectite (represented by beidellite), kaolinite and a metastable aluminosilicate such as halloysite (brackets denote activity). Dashed lines indicate that the exact solubility is highly uncertain but show the direction of change. The data for several HBN sites (Sagehen, CA (SHCA), Hayden Creek, ID (HCID) and Andrews Creek, WA (ACWA)) is plotted for comparison. The arrow shows the trajectory of the reactive transport model. The diagram is constructed assuming the log $[Ca]/[H^+]^2 = 16$.

for assessing restrictions on solute generation imposed by either chemical equilibrium or flow path lengths. Variations in water content and the boundary condition for PCO_2 impact both the final equilibrium concentrations and the equilibration length scale or equilibration time (Fig. 4A, B). In both cases, the evolution to different chemical endpoints is a result of differences in the final pH, as suggested by the activity diagram shown in Fig. 3. For unsaturated flow, the model PCO_2 is effectively constant throughout the profile, creating a competition between the dissolution of CO_2 into the pore water, which lowers the pH, and the feldspar hydrolysis reactions. The net result is an increase in equilibration length and equilibrium concentration with increasing PCO_2. This difference in chemical evolution emphasizes the strong coupling between hydrologic and biogeochemical processes—abiotic and biotic factors that influence soil water pH, including the presence of organic acids, are thus likely to strongly impact the extent of weathering. In contrast, changes in mineral surface area and porosity do not impact the final equilibrium concentration, just the length scale (Fig. 4C). Increases in mineral surface area decrease the equilibrium length scale because reaction rates increase. The reactive transport model also predicts longer times to reach equilibrium at lower temperatures due to slower reaction kinetics. This highlights the expansive set of variables that factor into the generation of solutes from weathering processes (Beaulieu et al., 2010; Berner, 1992; Bluth and Kump, 1994; Maher et al., 2009; Richards and Kump, 2003; West et al., 2005).

In general, parameters that slow the approach to equilibrium (e.g. reduced mineral surface area/reaction rate or increased flow rate) result in longer equilibration length scales. Parameters that change the composition of the system tend to change both the equilibrium length scale and the concentration (soil PCO_2 or pH, unsaturated flow, mineral solubilities and to some extent temperature). The reaction time in the unsaturated zone relative to the saturated zone will also be an important control on the equilibration length and concentration. The sensitivity analysis demonstrates that weathering evolution can still be effectively described by a theoretical equilibration length and equilibrium or endpoint concentration. The theoretical model equilibration lengths (0.5 to 3 m) are similar to those of soils and hillslopes. However, detailed field studies that assess equilibration

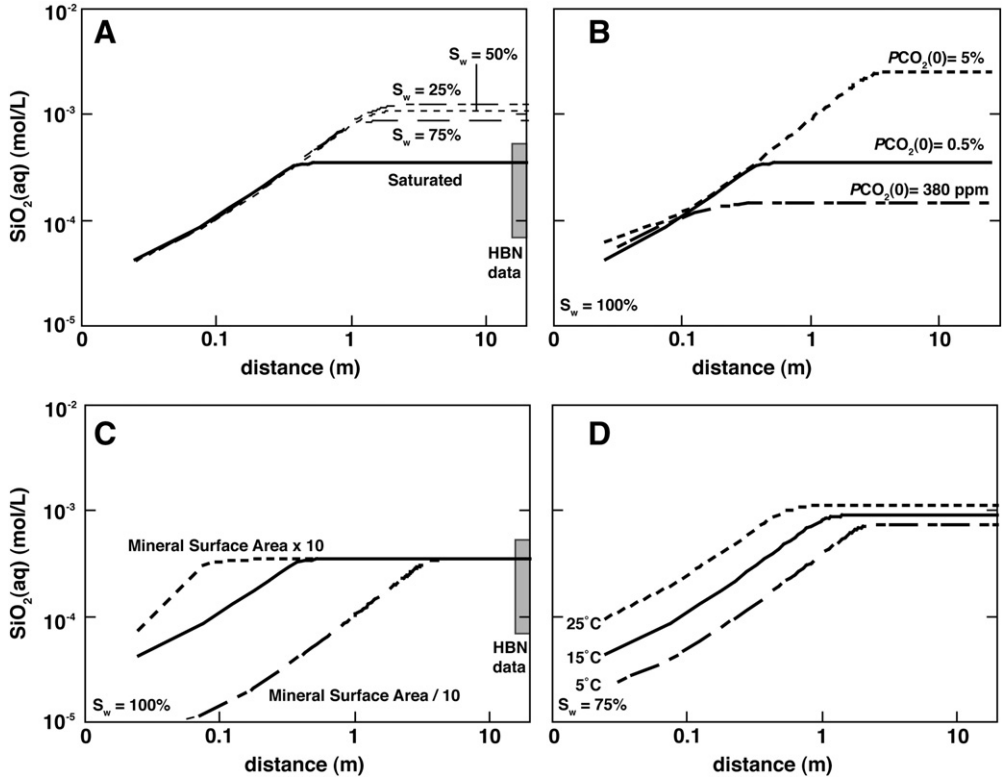

Fig. 4. Sensitivity of equilibrium Si concentrations and equilibration lengths to different assumptions based on numerical multi-component simulations. Flow rate is assumed to be 1 m/yr and temperature is 15 °C unless otherwise indicated. The bold line shows the reference model scenario which most closely reproduces the HBN river data. (A) Effect of changes in the liquid saturation (S_w) (or ratio of volumetric water content to porosity). (B) Effect of changes in mineral surface area. All mineral surface areas were scaled equally by a factor of 10. (C) Effect of initial soil PCO_2. (D) Effect of temperature for unsaturated flow conditions (saturated flow temperature dependence shown in Fig. 5). Note log scale on both axes. Shaded field corresponds to range of average values from HBN sites.

lengths and endpoints in tandem with the lithology, temperature and hydrology are critical for evaluating this approach.

3.2. Concentration as a function of temperature and fluid residence time

Fig. 5 shows the theoretical evolution of solute concentrations as a function of fluid residence time for different temperatures and saturated flow. The evolution of concentrations are similar across 2 orders of magnitude in flow rates (e.g. 0.1 to 10 m/yr) for a given temperature, suggesting that fluid residence time is a useful variable for understanding chemical evolution. The decreasing final concentration with increasing temperature predicted for fully saturated flow conditions is the reverse of the temperature dependence predicted for unsaturated flow in Fig. 4D. The difference is due to the presence of $CO_2(g)$ throughout the profile for unsaturated flow, compared to saturated flow where the amount of CO_2 dissolved in the water entering the profile is determined by the temperature and boundary condition for PCO_2 (which was held constant at 0.5% in both cases). As a result, for unsaturated flow both water flux and temperature impact the final equilibrium concentration. In reality, soil PCO_2 levels likely decrease with temperature due to lower biological productivity. In addition to the pH effects due to $CO_2(g)$ solubility and transport, temperature also impacts the reaction kinetics. For example, at short fluid residence times the concentration is greater at higher temperatures because of elevated reaction kinetics.

Between or within the six HBN catchments considered here, water composition show no consistent relationship to water temperature—some catchments show no correlation between concentration and temperature (SHCA, KMHI, HCID), while others show a weak positive correlation (ECCA) or a weak negative correlation (ACWA, WCMI)—likely because the effects of temperature are complicated by the flow conditions. Detailed field studies examining the dynamics of $CO_2(g)$ in the soil zone and the resulting impacts on solute generation would help to evaluate the actual relationship between temperature, equilibrium composition, extent of weathering and hydrologic conditions.

Many studies have assumed that silicate weathering reactions are slow relative to transport such that rates are kinetically- or surface-reaction controlled. Based on this assumption, equations have been developed that relate weathering fluxes to temperature (T) using the activation energy (E_a) according to the Arrhenius relationship: $k(T) = Ae^{(-Ea/RT)}$ where k is the weathering rate, A is the pre-exponential factor, R is the gas constant (Brady and Carroll, 1994; Clow and Mast, 2010; Velbel, 1993; White and Blum, 1995). Application of an Arrhenius-style relationship to weathering fluxes is empirical as it does not capture the mechanisms behind solute generation and is only valid if chemical conditions are far from equilibrium. Also, there is no maximum limit to concentrations. In contrast, it is clear from Fig. 5 that the approach to equilibrium and the equilibrium composition are important controls on solute fluxes. This behavior, and the variations in secondary phases and soil productivity (Curtis, 1990; Folkoff and Meentemeyer, 1985), may explain why it has been difficult to determine the temperature dependence of weathering rates across different environments (Hartmann et al., 2010; Millot et al., 2002, 2003).

3.3. Model for solute flux as a function of fluid residence time

More complex reactive transport approaches have been used to consider catchment- and global-scale chemical weathering (Beaulieu et al., 2010; Godderis et al., 2008; Roelandt et al., 2010; Violette et al., 2010). The challenge for more complex approaches is to parameterize large systems without making unsupported assumptions. An alternative approach is to develop scaling relationships that account for the key variables that control solute fluxes and test them against numerical models and well-studied systems. Results from the simplified model above suggest that the residence time of fluid relative to the residence time required to approach chemical equilibrium is the dominant control on solute fluxes. A simple model that uses only these parameters will be developed and compared to the reactive transport results and data from six HBN catchments.

The concentration of a dissolving solute, c, along a flow path (x) as a function of the flow rate (q[m/yr]), the volumetric water content (θ) and the net of the dissolution ($\sum R_{d,i}$ [mol/m^3-fluid/yr]) and precipitation ($\sum R_{p,I}$) rates summed over each mineral (i), can be described in simplified form as:

$$\frac{dc}{dt} = -\frac{q}{\theta}\frac{dc}{dx} + \sum_i \mu_i R_{d,i}\left(1-\left(\frac{c}{c_{eq}}\right)^{n_i}\right)^{m_i} - \sum_i \mu_i R_{p,i}\left(1-\left(\frac{c}{c_{eq}}\right)^{n_i}\right)^{m_i}. \quad (1)$$

The exponents n *and* m reflect the observation that the dissolution and precipitation behavior of many minerals exhibits a non-linear dependence on the departure from equilibrium (Hellmann and Tisserand, 2006) and μ_i is the stoichiometric coefficient. The value of c_{eq} reflects the equilibrium concentration where rates of dissolution and precipitation are zero, and reflects the decrease in rates as fluids approach equilibrium. The terms $R_{d,i}$ and $R_{p,i}$ are the product of the dissolution rate constant k_i (mol/m^2/s), the mineral surface area A_i (m^2/m^3-mineral), any term describing inhibition or activation, and the mineral to fluid ratio M (m^3-mineral/m^3-fluid). The dispersion term in Eq. (1) (not shown) is neglected for simplicity. After an initial relaxation time which is on the order of a year or less, the shape of the solute profile (dc/dx) should reach a quasi-steady state as long as mineral volumes are

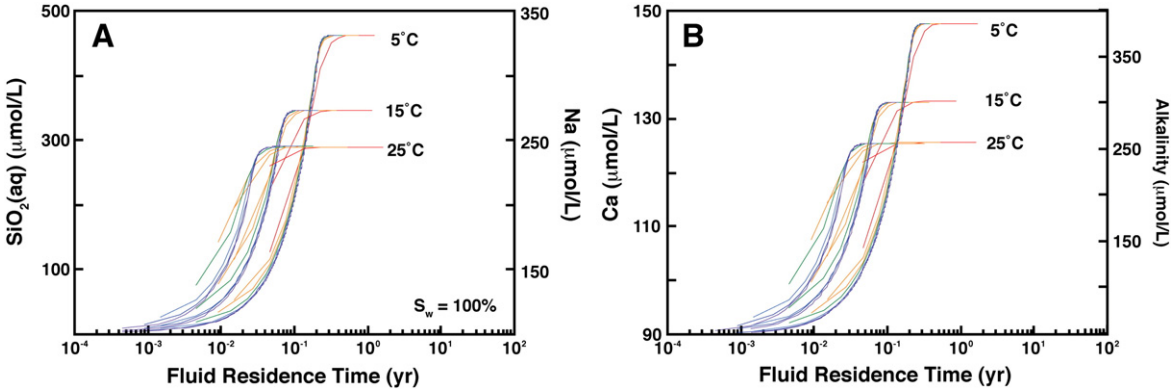

Fig. 5. (A) SiO_2(aq) and Na and (B) calcium and alkalinity (K and Al not shown) concentrations as a function of fluid residence times at different temperatures for a system of K-feldspar, plagioclase (An_{20}) and halloysite; The individual lines correspond to a range of flow rates from 0.1 m/yr to 10 m/yr showing the correspondence between fluid residence time and the evolution of concentration across flow rates. Simulations assume 100% liquid saturation. Minerals included in the simulation are plagioclase (An_{20}) (18.2 wt.%), K-feldspar (18.2 wt.%), quartz (60.6 wt.%), and halloysite (3.0 wt.%). Note the linear concentration scale on the y-axis and logarithmic scale on the x-axis.

changing slowly (ca. 10,000s of years) (Lichtner et al., 1986) so that the solute profile can be represented by:

$$\frac{dc}{dx} = \frac{\theta}{q}\sum_i \mu_i R_{d,i}\left(1-\left(\frac{c}{c_{eq}}\right)^{n_i}\right)^{m_i} - \frac{\theta}{q}\sum_i \mu_i R_{p,i}\left(1-\left(\frac{c}{c_{eq}}\right)^{n_i}\right)^{m_i} \quad (2)$$

Based on Eq. (2), the concentration gradient (dc/dx) depends on the balance between the flow rate and the reaction rates. Once the fluid has reached equilibrium (c_{eq}) with the dissolving and precipitating phases, dc/dx is zero and the maximum possible solute flux (F_{max}) is achieved ($F_{max} = qc_{eq}$). Until equilibrium is reached, the solute flux varies as a function of the flow rate and the concentration (Fig. 1B). Conceptually, this idea can be represented by considering the change in concentration as a function of the residence time of the fluid ($\tau_f = L\theta/q$) at distance L as shown in Fig. 5. If the fluid residences times are long enough that fluids reach equilibrium with the solids, the primary control on the solute flux is discharge.

In order to understand how solute fluxes vary with catchment fluid residence time, it is helpful to have an equation that predicts the solute curve shown in Figs. 4 and 5. This can be done by assuming that $\sum \mu_i R_{d,i} - \sum \mu_i R_{p,i}$ is equal to R_n, the net increase in solute, and solving for the concentration as a function of distance based on Eq. (2):

$$c(x) = c_0 \exp\left(\frac{-R_n\theta x}{qc_{eq}}\right) + c_{eq}\left(1-\exp\left(\frac{-R_n\theta x}{qc_{eq}}\right)\right). \quad (3)$$

where c_0 is the initial solute concentration at the inlet (nominally zero) and x, the distance along the flow path (c_{eq} and R_n are a function of temperature, composition (including mineral and gasses) and liquid saturation). This approximation assumes no net addition of solute from other sources along the flow path. Eqs. (2) and (3) could be amended if this assumption is violated. However, if all fluids are either equilibrated with the solids before they mix, or isolated from mixing in the subsurface, this assumption has a negligible effect on the composition of waters.

Eq. (3) can also be expressed in terms of fluid residence time ($\tau_f = L\theta/q$), if x is equal to the length scale of the system (L):

$$c(\tau_f) = c_0 \exp\left(\frac{-R_n\tau_f}{c_{eq}}\right) + c_{eq}\left(1-\exp\left(\frac{-R_n\tau_f}{c_{eq}}\right)\right) \quad (4)$$

Determining the effective net reaction rate for a natural system is challenging. However, a measure of the net reaction rate is the distance (or fluid residence time) required for the system to approach equilibrium. The ratio of c_{eq}/R_n is effectively a measure of the time required for the fluid to reach equilibrium, or the "equilibrium fluid residence time", τ_{eq}. As demonstrated in Figs. 4 and 5, τ_{eq} can vary depending on a number of factors, although timescales of months to years are within the range of median residence times for many catchments (McGuire and McDonnell, 2006; Stewart et al., 2010). Eq. (4), while simple, is consistent with the theoretical evolution of the system: as actual fluid residence times become large relative to the ratio of c_{eq}/R_n, the concentration approaches c_{eq} (Aagard and Helgeson, 1982; Lasaga and Rye, 1993; Steefel and Lasaga, 1994).

An alternative way to estimate the net reaction rate is to consider the ratio of the dissolution rate to the precipitation rate. Secondary minerals cannot precipitate more quickly than minerals dissolve so R_d/R_p must be close to 1. In the reactive transport simulations, R_d/R_p was between 1.66 and 1.76. Experimental batch studies also demonstrated a ratio of oligoclase dissolution to kaolinite precipitation of 1.62 (Zhu et al., 2010). Using this relationship, the equilibrium fluid residence time (τ_{eq}) is:

$$\tau_{eq} \approx \frac{c_{eq}}{R_n} \approx \frac{c_{eq}}{\varepsilon R_d} \quad (5)$$

where ε describes proportionality between net precipitation and dissolution rates and is likely on the order of 0.56 for Si when the stoichiometry (e.g. albite to halloysite) is accounted for. Using the data from the reactive transport model, c_{eq} at 15 °C is 348 μmol/L, R_d is 1.7×10^{-3} mol/L/yr, and τ_{eq} is equal to 0.3 yr, in agreement with the model profiles. If c_{eq}/R_d is assumed to be proportional to the fluid residence time where the system reaches equilibrium (τ_{eq}), Eq. (4) can be recast to describe the change in concentration along a flow path as a function of the ratio of the actual fluid residence time to the fluid residence time required for the system to approach equilibrium:

$$c(\tau_f) = c_0 \exp\left(\frac{-\tau_f}{\omega\tau_{eq}}\right) + c_{eq}\left(1-\exp\left(\frac{-\tau_f}{\omega\tau_{eq}}\right)\right) \quad (6)$$

A scaling factor (ω) is introduced to control where the concentration approaches equilibrium relative to the equilibrium fluid residence time such that $\omega = -\ln(1-f)$ where f is the fraction of the equilibrium concentration achieved. Values for f and ω are assumed to be 0.9 and 2.3 respectively. In Fig. 6, Eq. (6) is compared to the results from the reactive transport simulations for saturated flow assuming the same equilibrium concentrations and fluid residence times.

The equilibrium fluid residence time is a measureable parameter that reflects the combined influence of multiple factors, including mineral surface areas, temperature, mineral solubility, biological productivity and hydrologic properties. The τ_{eq} is thus likely to vary widely between lithologies, climates and ecosystems and may be difficult to estimate *a priori*, but could be assessed through geochemical measurements. This equation predicts a similar behavior to that of Scanlon et al. (2001), although it is applicable over a broader range of fluid residence times and predicts a maximum concentration that is dependent on the composition of the system. The reactive transport simulations included multiple phases and reaction kinetics with a non-linear dependence on reaction affinity. As a result, Eq. (6) reproduces the general profiles but departs from the numerical model near equilibrium. Overall, this approach captures the evolution of the solute profile determined by the numerical model without relying on strictly empirical parameters. Eq. (6) is not a perfect representation of a multi-component reactive transport system, but it is simple and relies on measureable parameters and may thus offer a useful interpretive tool that could be strengthened by further comparisons to well-studied catchments.

4. Discussion

The reactive transport model approach provides a framework for understanding how different variables may influence the generation

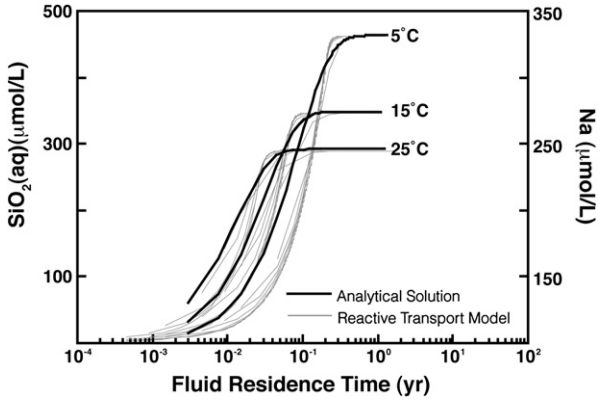

Fig. 6. Comparison between numerical model and analytical model (Eq. (6)) for Si and Na assuming equilibrium fluid residence time (τ_f) and concentrations (c_{eq}) from the model profiles in Fig. 5.

of solutes and control chemical fluxes from landscapes. This framework was used to generate a simple model based on scaling arguments that captures the primary variables. An additional utility of a simple model is that variables can be determined for individual catchments without relying on empirical parameters.

The model analysis suggests that the primary controls on weathering fluxes are the residence time of water in the saturated and unsaturated zones, mineral surface areas and solubilities and the dynamics of CO_2 production and transport. These factors, along with temperature, control the rate of approach to chemical equilibrium and the final chemical equilibrium concentration, which in turn determine the maximum solute flux. The fact that individual catchments show less variability in concentration than discharge may result from equilibrium controls (or long fluid residence times such that the maximum solute concentration is reached before the fluids reach the channel). This is consistent with a number of studies that have proposed that Si concentrations are controlled by metastable amorphous aluminosilicates (Clow and Mast, 2010; Garrels and Mackenzie, 1967; Stefansson and Gislason, 2001).

4.1. Importance of catchment residence time distribution

The previous discussion has focused on the evolution of solutes along a 1-dimensional flow path with no mixing, but in reality catchments are comprised of a distribution of flow paths and fluid residence times. Given the importance of fluid transit through catchments, considerable effort has been devoted to measuring the mean residence time (τ_m) of water. The mean fluid residence time reflects the distribution of travel times for water between the point of infiltration and the channel, and is known to influence both the shape of the hydrograph and the fate and transport of solutes. A number of studies have considered the relationship between landscape characteristics and mean residence time, but as of yet no direct scaling relationship has emerged that is applicable from basin to basin (Tetzlaff et al., 2009).

As a result of the distribution of fluid residence times some waters in a catchment will have spent enough time in the subsurface to equilibrate, while others may not have approached equilibrium. The distribution of fluid residence times is thus important when considering the application of Eq. (6) to catchments. The distribution of fluid transit times $h(\tau_f)$ within small catchments (first or second order) is most commonly described as an exponential function (McGuire and McDonnell, 2006):

$$h\left(\tau_f\right) = \frac{1}{\tau_f}\exp\left(-\tau_f/\tau_m\right) \tag{7}$$

However, recent studies have suggested that a gamma distribution may be a better empirical representation of residence times (Kirchner et al., 2000; 2001; McGuire et al., 2005):

$$h\left(\tau_f\right) = \frac{\tau_f^{\alpha-1}}{\beta^{\alpha}\Gamma(\alpha)}\exp\left(-\tau_f/\beta\right) \tag{8}$$

In Eqs. (7) and (8) τ_m is the mean residence time and α is the shape factor, which influences the shape of the distribution and extent of tailing. The other factors in the gamma distribution are the scale factor $\beta(=\tau_m/\alpha)$ and the gamma function $\Gamma(\alpha)$ Other approaches for catchment transit time distributions have included the sine-wave, piston flow and binomial models. Recent studies have found that the gamma distribution (with α~0.5) reproduced the power spectral scaling observed in some catchments better than the exponential model (Godsey et al., 2010). In addition, a recent comparison between transit times measured with either stable isotopes ($\delta^{18}O$, δD) and/or tritium (^3H) suggests that stable isotope approaches are biased towards shorter mean residence time estimates because waters older than about 4 years no longer show detectable variation in $\delta^{18}O$, δD (Stewart et al., 2010). Old ground water components reflective of deep storage can be a substantial fraction of the discharge in headwater catchments, while mean residence times and ground water components of large rivers are potentially even greater (Rice and Hornberger, 1998; Scanlon et al., 2001). For example, 60% of the flow in the Ohio River is groundwater with a mean residence time of 10 years, while 90% of the flow in the Missouri River is groundwater with τ_m of 4 years (Michel, 2004). Most importantly, the large contributions of groundwater and mean residence times on the orders of months to years suggests that for many catchments subsurface contact time is sufficient for chemical equilibration, in contrast to other studies which assume chemical equilibrium is unlikely.

The effect of a distribution of fluid residence times on river solute concentrations is shown in Fig. 7 for both the exponential and gamma distributions assuming Eq. (6). The fluid residence time required to reach equilibrium is assumed to be 1 year and the equilibrium concentration is 350 μmol/L. Compared to a homogenous flow path, the concentrations are lower for all distributions because the packets of fluid with residence times less than 1 year do not equilibrate with the solids. The lowest concentration occurs for the gamma distribution with $\alpha = 0.25$ because the distribution is highly skewed towards shorter residence times and less reaction. The exponential and gamma distributions with a higher α value more closely approach the case for a single flow path. Seasonal or event-driven shifts in fluid residence time may not appreciably affect the concentration of discharge as long as τ_m remains greater than τ_{eq}. Conversely, if τ_m is shorter than τ_{eq} waters may show considerable variability in Si and other weathering derived solutes—heterogeneity in flow paths can have a substantial impact on concentrations of a reacting solute. This analysis suggests that the average dimensions and flow routing of catchments will strongly determine the solute flux from weathering.

The effect of basin size was also observed by Wolock et al. (1997), where base cation concentrations, acid neutralizing capacity and pH varied sharply as basin size increased to 3 km^2, but showed small to no variations with additional increases in size. An increase in solute flux with increasing basin size and/or the transition from mountainous regions to alluvial plains was also observed for both the Ganges Basin (West et al., 2002) and the Mackenzie River (Lemarchand and Gaillardet, 2006; Millot et al., 2003). These observations, which are supported by the model, suggest that the factors controlling solute fluxes may change with the scale of observation.

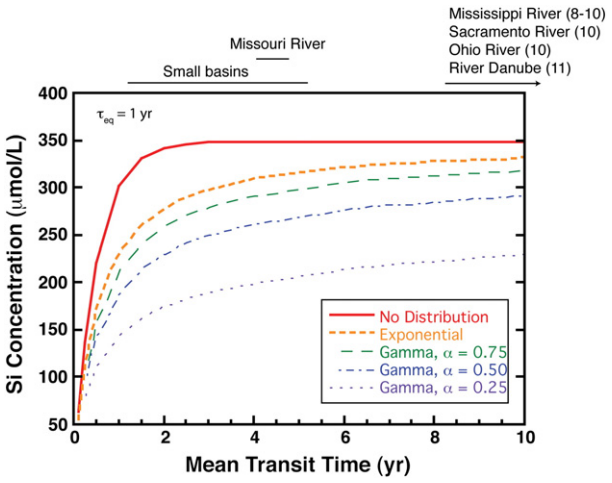

Fig. 7. Model predicted Si concentrations for different fluid residence time distributions (see text for description of models). The exponential and gamma models are equivalent when $\alpha = 1$. Range of mean transit times measured for small basins is summarized from McGuire and McDonnell (2006) and Stewart et al. (2010) and references therein. Also shown are mean transit time for the Missouri and Ohio Rivers (Michel, 2004), Sacramento and Mississippi Rivers (Michel, 1992) and the Danube River (Yurtsever, 1999). Numbers in parenthesis correspond to the measured mean transit time in years.

4.2. Concentration–discharge relationships of individual catchments

Small changes in the concentration of waters over large changes in discharge as observed in many catchments (*cf.* Godsey et al., 2009) could occur in systems where fluid residence times exceed the time required to approach equilibrium. "Chemostatic" behavior is thus attributed here to chemical equilibrium between primary and secondary phases, and most likely a poorly crystalline precursor phase. Fig. 8 shows the model fit to the data for six HBN catchments with different discharge–concentration patterns using Eq. (6). Each catchment was fit by varying the ratio of the product of the path length and the porosity, $L\theta$ (=m) to the equilibrium fluid residence time (τ_{eq}) so that $L\theta/\tau_{eq}$ (=m/yr) is the actual adjustable parameter because true equilibrium length scales are not known. Thus, the ratio of the fluid residence time to the equilibrium fluid residence time varies with discharge.

As the general relationship between concentration and fluid residence time does not change appreciably when the distribution of fluid residence time is considered, a mean flow path length is assumed. For the Type 1 catchments, Sagehen Creek, in the Sierra Nevada Mountains (SHCA) and Kahakuloa Stream, Hawaii (KMHI), no plateau is apparent so the Si concentration at low discharge is assumed to represent the equilibrium concentration (Fig. 8A, B). To fit Sagehen Creek also required that the initial concentration was elevated (260 μmol/L). Sagehen Creek is dominated by spring snow melt and fracture-controlled perennial springs with residence times on the order of decades (Rademacher et al., 2005), so the value for the initial concentration may reflect spring input which would not vary with discharge. For all of the other catchments the initial concentration was zero.

For Type 2 or "chemostatic" catchments, the $L\theta/\tau_{eq}$ values are minimum values (Fig. 8C, D). The Type 3 catchments, which show a chemostatic behavior only at low discharge (Andrews Creek in the

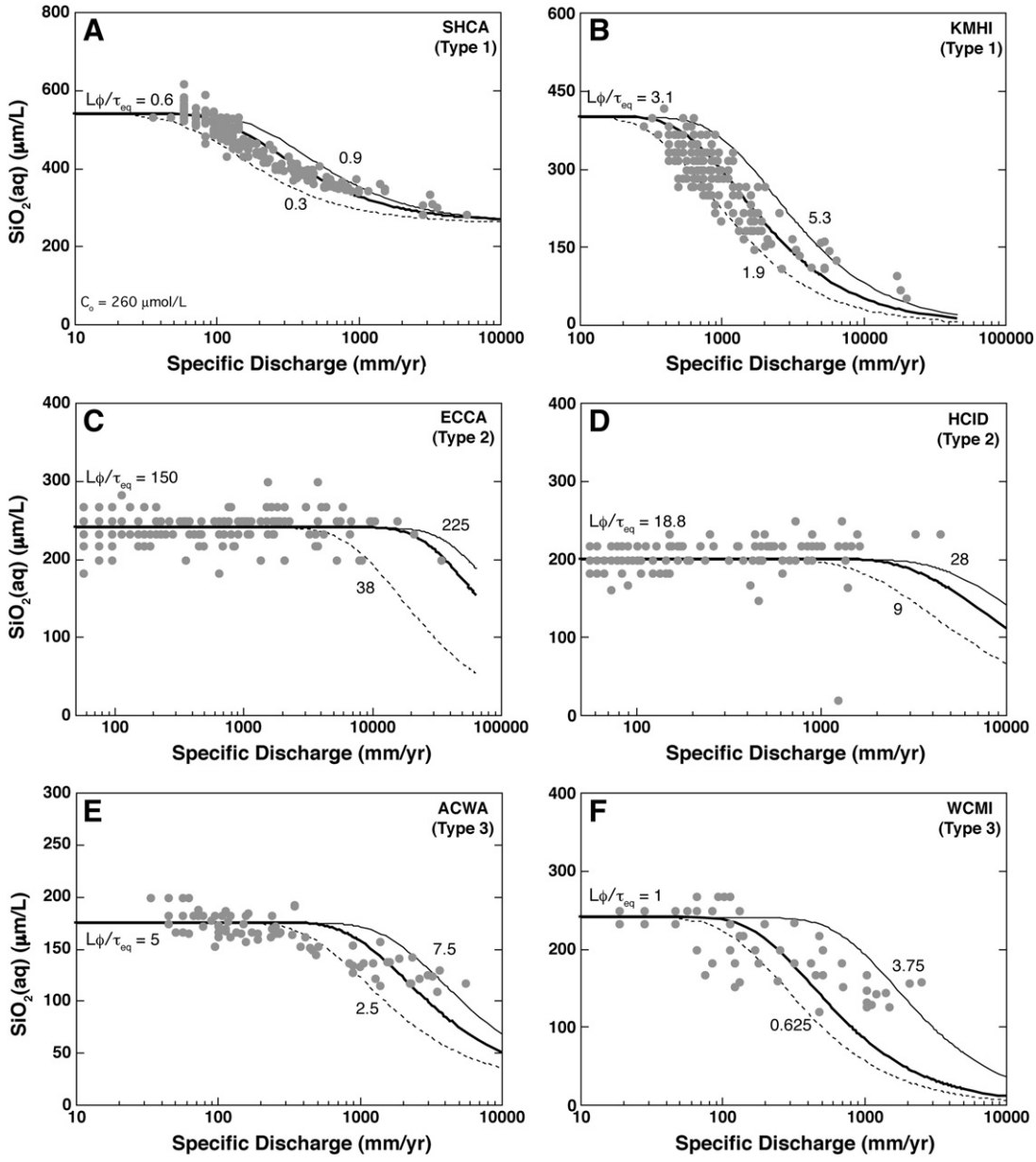

Fig. 8. Model fit to catchment concentration–discharge data for six HBN sites showing fir to type 1 (A, B), type 2 (C, D) and type 3 (E, F) relationships. Discharge data is normalized to the catchment area reported in Mast and Clow (2000). Data points correspond to individual measurements where both concentration and discharge were recorded. The equilibrium fluid residence time (τ_{eq}) for all cases is 0.08 years. (A) Sagehen Creek, CA (SHCA). (B) Kahakuloa Stream, HI (HCID). (C) Elder Creek, CA (ECCA). (D) Hayden Creek, ID (HCID). (E) Andrews Creek, WA (ACWA). (F) Washington Creek, MI (WCMI). All initial concentrations (C_0) were equal to zero in the model, with the exception of Sagehen Creek, CA.

Cascade Mountains of Washington (ACWA) and Washington Creek in Michigan (WCMI)), the concentration plateau is assumed to represent the equilibrium concentration (Fig. 8E, F). In general, the $L\theta/\tau_{eq}$ values are greatest for the chemostatic catchments, as expected. The value of τ_{eq} (0.08 years) is likely a minimum value — τ_{eq} values for the Santa Cruz marine chronosequence are closer to 1 to 2 years (Maher et al., 2009). $L\theta$ also cannot be directly estimated for HBN catchments because it reflects the combined soil thickness and hillslope length. Given these uncertainties and the possibility that τ_{eq} varies between catchments, it is difficult to assess whether the predicted $L\theta$ values are reasonable. Assuming τ_{eq} is between 0.08 and 1 year, $L\theta$ values would range from 0.5 to 12 m to 0.63 to 150 m respectively, values that are generally consistent with hillslope length scales. A potentially useful outcome of the model is that if τ_{eq} is known, concentration–discharge data can be used to determine average flow path lengths and porosity. The ability to describe different types of concentration–discharge patterns also emphasizes the importance of a mixed-equilibrium kinetic framework for interpreting chemical weathering processes. However, although the simple model provides a useful approach for describing different concentration–discharge relationships, it still requires testing and refinement at sites with well-defined hydrologic systems and detailed compositional data (e.g. knowledge of soil and groundwater flow paths and water fluxes, primary and secondary mineral distributions, solute and reaction affinity gradients along flow paths, and discharge–concentration or discharge–reaction affinity relationships for stream waters). Comparisons between the simple model framework and detailed catchment-scale reactive transport models (e.g. Godderis et al., 2009; Violette et al., 2010) may also help to refine the scaling relationships defined here so that they can be applied with more confidence to less monitored catchments, or potentially up-scaled to describe large rivers.

4.3. Topographic controls on solute fluxes

Topography is known to be an important control on the movement of water through a basin (Beven, 1987; Tetzlaff et al., 2009) and on solute fluxes (Millot et al., 2003; Stallard and Edmond, 1983; West et al., 2002; West et al., 2005; Wolock et al., 1997). The primary role of topography as considered here is to determine the mean fluid residence time relative to the equilibrium fluid residence time. As basin scale increases, the evolution of catchment geomorphology may lead to changes in the dynamics of hydrologic processes. Larger basins favor longer flow paths, longer fluid residence times and thus potentially the highest specific solute fluxes. Erosional processes may influence both the thickness of soils and the supply of fresh mineral (Waldbauer and Chamberlain, 2005), which would influence the fluid residence time and the equilibration time, respectively. For smaller basins with the same runoff and soil thickness, a larger fraction of the flow paths may not allow for equilibrium to be reached, resulting in lower fluxes (e.g. Fig. 7). It may not necessarily be the overall size of the basin, but rather the geometry or "wavelength" of the drainage network that determines solute fluxes. In any case, the physical and chemical compositions and length scales of sub-basins within a catchment are an important control on solute fluxes.

Basin relief will also be an important parameter. As relief increases, the hydraulic gradient also becomes steeper resulting in shorter fluid residence times (Beven, 1987; Tetzlaff et al., 2009). If the transit time through the unsaturated zone is small relative to the overall transit time of water, the hydraulic conductivity [K_{ave} (m/day)], effective porosity ($\phi_{effective}$) and the hydraulic gradient determine the flow of water. If the hydraulic gradient approximates the topography, then the residence time along a flow path can be expressed as a balance between the hydraulic conductivity, the relief and the length scales:

$$\tau_c = \frac{\phi_{effective}(\Delta l_c)^2}{K_{ave}\Delta h} \quad (9)$$

where Δl_c is the distance from recharge to discharge (m) and Δh is the change in hydraulic head (m) along the flow path which should be proportional to the relief. As the ratio of $\phi_{effective}/K_{ave}$ is unlikely to vary substantially, the length scale and hydraulic gradient should be an important determinant of fluid residence times, along with soil structure. Topographic control of solute fluxes is probably weakest in areas where less permeable soils give rise to overland flow because residence times are effectively shorter. These areas include steep bedrock-dominated regions where soil production cannot keep pace with erosion, and more subdued deeply weathered lowlands with poor drainage. Deeply weathered areas may also have very long equilibrium fluid residence times, also weakening topographic effects.

High relief also tends to increase the length of valleys, the spacing between valleys and potentially the area of basins, extending the length of flow paths (Perron et al., 2008). Longer flow paths would increase solute fluxes for a given runoff as long as overland flow is not substantial. If longer flow paths are associated with high physical erosion rates, this may in part explain the correlation observed between weathering fluxes and physical erosion rates (Gaillardet et al., 1999; Hren et al., 2007; Waldbauer and Chamberlain, 2005). However, if increasing relief steepens the hydraulic gradient and shortens fluid residence time, then shorter residence times may result in lower concentrations. In any case, the characteristic length scale of the topography is likely to exert a strong control on the solute flux of a river.

5. Conclusions

The framework presented here suggests that both thermodynamic and hydrologic properties limit the solute fluxes carried by rivers. The thermodynamic limit is set by chemical equilibrium, where the maximum solute flux occurs when the system reaches equilibrium between the dominant primary and secondary phases. The hydrologic limit determines the time available for the fluid to react: the maximum solute flux occurs when fluid residence times allow for the equilibrium limit to be maintained. The thermodynamic and hydrologic scales are connected by the relationship between the equilibrium concentration and the time required for a system to reach the equilibrium concentration.

Evaluating the concentration–discharge patterns of rivers can also suggest how solute fluxes might respond to changes in climate or topography. In Fig. 9, the model concentrations are converted to fluxes and compared to the data for two catchments, ECCA (Type 2) and

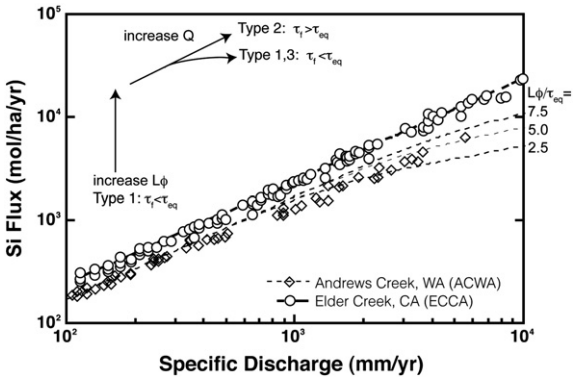

Fig. 9. Comparison between measured and model Si fluxes as a function of specific discharge (Q) for two catchments from Fig. 8: a chemostatic (type 2) catchment (Elder Creek, CA) and a catchment with decreasing concentration above a threshold in discharge (type 3) (Andrews Creek, WA). Thick solid line is the best fit for ECCA and thin dashed lines are the range of model values for ACWA, both model fits are from Fig. 8. Schematic arrows depict how the weathering flux varies with discharge according to the ratio of fluid residence time (τ_f) to equilibrium fluid residence time (τ_{eq}) resulting in the different types of concentration–discharge behavior. Curves corresponding to variations in $L\phi/\tau_{eq}$ for ACWA are shown for reference.

ACWA (Type 3). The inset diagram suggests how solute fluxes could change with the evolution of climate and topography. "Chemostatic" or Type 2 catchments reflect the maximum concentration and thus solute flux depends on discharge. Unless the equilibrium endpoint changes, Type 2 catchments can be considered as optimized systems. In contrast, for Type 1 and 3 systems where residence times are short ($\tau_f < \tau_{eq}$), increasing flow path length would allow waters more time to react and thus become Type 2 systems. However, as runoff increases, if the length scales of the drainage are not sufficient to maintain equilibrium, then concentrations will decrease (e.g. Type 3 behavior). Changes in discharge of 10 to 40% in response to climate change (IPCC, 2007) may not result in proportional increases in solute and alkalinity fluxes if the fluid residence times of catchments become too short or the equilibrium endpoints and length scales change due to temperature/PCO_2 effects.

Over geologic timescales, if major rivers of the world all contain waters reacted to the thermodynamic maximum then the primary determinant of global solute fluxes is runoff. Alternatively, increasing the thermodynamic maximum by reducing the water saturation of soils and increasing subsurface $CO_2(g)$ will elevate solute fluxes in basins with fluid residence times long enough to equilibrate to the new potential maximum. In contrast, if the waters of major rivers are not reacted to the full extent, then increasing flow path length will drive solute fluxes higher as the fluids have more opportunity to react. Assuming the equilibrium concentrations are fixed, shifts in global solute fluxes may require that both the length scales and the runoff of basins increase in tandem, changes that commonly occur in response to mountain building.

Acknowledgments

This research was supported by Stanford University. C. R. Lawrence, J. Gaillardet, C. P. Chamberlain, A. J. West and one anonymous reviewer are acknowledged for their insightful comments and discussions that greatly improved this manuscript.

References

Aagard, P., Helgeson, H.C., 1982. Thermodynamic and kinetic constraints on reaction-rates among minerals and aqueous-solutions .1. Theoretical considerations. Am. J. Sci. 282 (3), 237–285.

Anderson, S.P., Dietrich, W.E., Torres, R., Montgomery, D.R., Loague, K., 1997a. Concentration–discharge relationships in runoff from a steep, unchanneled catchment. Water Resour. Res. 33 (1), 211–225.

Anderson, S.P., Dietrich, W.E., Montgomery, D.R., Torres, R., Conrad, M.E., Loague, K., 1997b. Subsurface flow paths in a steep, unchanneled catchment. Water Resour. Res. 33 (12), 2637–2653.

Arnorsson, S., Stefansson, A., 1999. Assessment of feldspar solubility constants in water in the range 0 degrees to 350 degrees C at vapor saturation pressures. Am. J. Sci. 299 (3), 173–209.

Arvidson, R.S., Mackenzie, F.T., Guidry, M., 2006. MAGic: a Phanerozoic model for the geochemical cycling of major rock-forming components. Am. J. Sci. 306 (3), 135–190.

Asano, Y., Uchida, T., Ohte, N., 2002. Residence times and flow paths of water in steep unchannelled catchments, Tanakami, Japan. J. Hydrol. 261 (1–4), 173–192.

Beaulieu, E., Godderis, Y., Labat, D., Roelandt, C., Oliva, P., Guerrero, B., 2010. Impact of atmospheric CO_2 levels on continental silicate weathering. Geochem. Geophys. Geosyst. 11 (7), Q07007.

Berner, R.A., 1978. Rate control of mineral dissolution under earth surface conditions. Am. J. Sci. 278 (9), 1235–1252.

Berner, R.A., 1992. Weathering, plants, and the long-term carbon-cycle. Geochim. Cosmochim. Acta 56 (8), 3225–3231.

Berner, R.A., Kothavala, Z., 2001. GEOCARB III: a revised model of atmospheric CO_2 over Phanerozoic time. Am. J. Sci. 301 (2), 182–204.

Beven, K., 1987. Towards the use of catchment geomorphology in flood frequency predictions. Earth Surf. Process. Landforms 12 (1), 69–82.

Bluth, G.J.S., Kump, L.R., 1994. Lithologic and climatic controls of river chemistry. Geochim. Cosmochim. Acta 58 (10), 2341–2359.

Bowser, C.J., Jones, B.F., 2002. Mineralogic controls on the composition of natural waters dominated by silicate hydrolysis. Am. J. Sci. 302 (7), 582–662.

Brady, P.V., Carroll, S.A., 1994. Direct effects of CO_2 and temperature on silicate weathering: possible implications for climate control. Geochim. Cosmochim. Acta 58 (8), 1853–1856.

Chadwick, O.A., Chorover, J., 2001. The chemistry of pedogenic thresholds. Geoderma 100 (3–4), 321–353.

Clow, D.W., Mast, M.A., 2010. Mechanisms for chemostatic behavior in catchments: implications for CO_2 consumption by mineral weathering. Chem. Geol. 269 (1–2), 40–51.

Curtis, C.D., 1990. Aspects of climatic influence on the clay mineralogy and geochemistry of soils, paleosols and clastic sedimentary rocks. J. Geol. Soc. 147, 351–357.

Dessert, C., Dupre, B., Gaillardet, J., Francois, L.M., Allegre, C.J., 2003. Basalt weathering laws and the impact of basalt weathering on the global carbon cycle. Chem. Geol. 202 (3–4), 257–273.

Drever, J.I., Zobrist, J., 1992. Chemical weathering of silicate rocks as a function of elevation in the southern Swiss Alps. Geochim. Cosmochim. Acta 56 (8), 3209–3216.

Evans, C., Davies, T.D., 1998. Causes of concentration/discharge hysteresis and its potential as a tool for analysis of episode hydrochemistry. Water Resour. Res. 34 (1), 129–137.

Folkoff, M.E., Meentemeyer, V., 1985. Climatic control of the assemblages of secondary clay minerals in the A-horizon of United States soils. Earth Surf. Process. Landforms 10 (6), 621–633.

Gaillardet, J., Dupre, B., Louvat, P., Allegre, C.J., 1999. Global silicate weathering and CO_2 consumption rates deduced from the chemistry of large rivers. Chem. Geol. 159 (1–4), 3–30.

Garrels, R.M., Mackenzie, F.T., 1967. Origin of chemical compositions of some springs and lakes. Adv. Chem. Ser. (67), 222–242.

Gautier, J.M., Oelkers, E.H., Schott, J., 1994. Experimental study of K-feldspar dissolution rates as a function of chemical affinity at 150 °C and pH 9. Geochim. Cosmochim. Acta 58 (21), 4549–4560.

Godderis, Y., Donnadieu, Y., Tombozafy, M., Dessert, C., 2008. Shield effect on continental weathering: implication for climatic evolution of the Earth at the geological timescale. Geoderma 145 (3–4), 439–448.

Godderis, Y., Roelandt, C., Schott, J., Pierret, M.C., Francois, L.M., 2009. Towards an integrated model of weathering, climate, and biospheric processes, in Thermodynamics and Kinetics of Water–Rock Interaction. Rev. Mineral. 70, 411–434.

Godsey, S.E., Kirchner, J.W., Clow, D.W., 2009. Concentration–discharge relationships reflect chemostatic characteristics of US catchments. Hydrol. Process. 23 (13), 1844–1864.

Godsey, S.E., et al., 2010. Generality of fractal 1/f scaling in catchment tracer time series, and its implications for catchment travel time distributions. Hydrol. Process. 24 (12), 1660–1671.

Hartmann, J., Jansen, N., Durr, H.H., Harashima, A., Okubo, K., Kempe, S., 2010. Predicting riverine dissolved silica fluxes to coastal zones from a hyperactive region and analysis of their first-order controls. Int. J. Earth Sci. 99 (1), 207–230.

Hellmann, R., Tisserand, D., 2006. Dissolution kinetics as a function of the Gibbs free energy of reaction: an experimental study based on albite feldspar. Geochim. Cosmochim. Acta 70 (2), 364–383.

Hornberger, G.M., Scanlon, T.M., Raffensperger, J.P., 2001. Modelling transport of dissolved silica in a forested headwater catchment: the effect of hydrological and chemical time scales on hysteresis in the concentration–discharge relationship. Hydrol. Process. 15 (10), 2029–2038.

Hren, M.T., Hilley, G.E., Chamberlain, G.P., 2007. The relationship between tectonic uplift and chemical weathering rates in the Washington Cascades: field measurements and model predictions. Am. J. Sci. 307 (9), 1041–1063.

IPCC, C.W.T., 2007. Climate Change 2007: Synthesis Report. In: Pachauri, R.K., Reisinger, A. (Eds.), Contribution of Working Groups I, II and III to the Fourth Assessment Report of the Intergovernmental Panel on Climate Change. IPCC, Geneva, Switzerland, p. 104.

Johnson, N.M., Likens, G.E., Bormann, F.H., Fisher, D.W., Pierce, R.S., 1969. A working model for variation in stream water chemistry at Hubbard Brook Experimental Forest, New Hampshire. Water Resour. Res. 5 (6), 1353–1363.

Kirchner, J.W., Feng, X.H., Neal, C., 2000. Fractal stream chemistry and its implications for contaminant transport in catchments. Nature 403 (6769), 524–527.

Kirchner, J.W., Feng, X.H., Neal, C., 2001. Catchment-scale advection and dispersion as a mechanism for fractal scaling in stream tracer concentrations. J. Hydrol. 254 (1–4), 82–101.

Lasaga, A.C., Rye, D.M., 1993. Fluid-flow and chemical-reaction kinetics in metamorphic systems. Am. J. Sci. 293 (5), 361–404.

Lasaga, A.C., Soler, J.M., Ganor, J., Burch, T.E., Nagy, K.L., 1994. Chemical-weathering rate laws and global geochemical cycles. Geochim. Cosmochim. Acta 58 (10), 2361–2386.

Lemarchand, D., Gaillardet, J., 2006. Transient features of the erosion of shales in the Mackenzie Basin (Canada), evidences from boron isotopes. Earth Planet. Sci. Lett. 245 (1–2), 174–189.

Lichtner, P.C., Oelkers, E.H., Helgeson, H.C., 1986. Exact and numerical solutions to the moving boundary problem resulting from reversible heterogeneous reactions and aqueous diffusion in a porous-medium. J. Geophys. Res. Solid Earth Planets 91 (B7), 7531–7544.

Ludwig, W., Amiotte-Suchet, P., Munhoven, G., Probst, J.L., 1998. Atmospheric CO_2 consumption by continental erosion: present-day controls and implications for the Last Glacial Maximum. Glob. Planet. Chang. 17, 107–120.

Maher, K., 2010. The dependence of chemical weathering rates on fluid residence time. Earth Planet. Sci. Lett. 294 (1–2), 101–110.

Maher, K., Steefel, C.I., DePaolo, D.J., Viani, B.E., 2006. The mineral dissolution rate conundrum: Insights from reactive transport modeling of U isotopes and pore fluid chemistry in marine sediments. Geochim. Cosmochim. Acta 70 (2), 337–363.

Maher, K., White, A.F., Steefel, C.I., Stonestrom, D.A., 2009. The role of secondary minerals and reaction affinity in regulating weathering rates at the Santa Cruz Marine Terrace Chronosequence. Geochim. Cosmochim. Acta 73, 2804–2831.

Mast, M.A., Clow, D.W., 2000. Environmental Characteristics and Water Quality of Hydrologic Benchmark Network Stations in the Western United States, 1963–1995*Rep*. USGS, Reston VA. 114 pp.
McDonnell, J.J., et al., 2010. How old is stream water? Open questions in catchment transit time conceptualization, modelling and analysis. Hydrol. Process. 24 (12), 1745–1754.
McGuire, K.J., McDonnell, J.J., 2006. A review and evaluation of catchment transit time modeling. J. Hydrol. 330 (3–4), 543–563.
McGuire, K.J., McDonnell, J.J., 2010. Hydrological connectivity of hillslopes and streams: characteristic time scales and nonlinearities. Water Resour. Res. 46.
McGuire, K.J., DeWalle, D.R., Gburek, W.J., 2002. Evaluation of mean residence time in subsurface waters using oxygen-18 fluctuations during drought conditions in the mid-Appalachians. J. Hydrol. 261 (1–4), 132–149.
McGuire, K.J., McDonnell, J.J., Weiler, M., Kendall, C., McGlynn, B.L., Welker, J.M., Seibert, J., 2005. The role of topography on catchment-scale water residence time. Water Resour. Res. 41 (5).
McGuire, K.J., Weiler, M., McDonnell, J.J., 2007. Integrating tracer experiments with modeling to assess runoff processes and water transit times. Adv. Water Resour. 30 (4), 824–837.
Michel, R.L., 1992. Residence times in river basins as determined by analysis of long-term tritium records. J. Hydrol. 130 (1), 367–378.
Michel, R.L., 2004. Tritium hydrology of the Mississippi River basin. Hydrol. Process. 18 (7), 1255–1269.
Millot, R., Gaillardet, J., Dupre, B., Allegre, C.J., 2002. The global control of silicate weathering rates and the coupling with physical erosion: new insights from rivers of the Canadian Shield. Earth Planet. Sci. Lett. 196 (1–2), 83–98.
Millot, R., Gaillardet, J., Dupre, B., Allegre, C.J., 2003. Northern latitude chemical weathering rates; clues from the Mackenzie River basin, Canada. Geochim. Cosmochim. Acta 67 (7), 1305–1329.
Oelkers, E.H., Schott, J., Devidal, J.L., 1994. The effect of aluminum, pH, and chemical affinity on the rates of aluminosilicate dissolution reactions. Geochim. Cosmochim. Acta 58 (9), 2011–2024.
Palandri, J.L., Kharaka, Y.K., 2004. A compilation of rate parameters of water–mineral interaction kinetics for application to geochemical modeling *Rep. 2004–1068*. US Geol. Surv. Open File Rep.
Perron, J.T., Dietrich, W.E., Kirchner, J.W., 2008. Controls on the spacing of first-order valleys. J. Geophys. Res. Earth Surf. 113 (F4).
Rademacher, L.K., Clark, J.F., Clow, D.W., Hudson, G.B., 2005. Old groundwater influence on stream hydrochemistry and catchment response times in a small Sierra Nevada catchment: Sagehen Creek, California. Water Resour. Res. 41 (2).
Rice, K.C., Hornberger, G.M., 1998. Comparison of hydrochemical tracers to estimate source contributions to peak flow in a small, forested, headwater catchment. Water Resour. Res. 34 (7), 1755–1766.
Richards, P.L., Kump, L.R., 2003. Soil pore-water distributions and the temperature feedback of weathering in soils. Geochim. Cosmochim. Acta 67 (20), 3803–3815.
Roelandt, C., Godderis, Y., Bonnet, M.P., Sondag, F., 2010. Coupled modeling of biospheric and chemical weathering processes at the continental scale. Global Biogeochem. Cycles 24.
Scanlon, T.M., Raffensperger, J.P., Hornberger, G.M., 2001. Modeling transport of dissolved silica in a forested headwater catchment: implications for defining the hydrochemical response of observed flow pathways. Water Resour. Res. 37 (4), 1071–1082.
Schott, J., Pokrovsky, O.S., Oelkers, E.H., 2009. The link between mineral dissolution/precipitation kinetics and solution chemistry, in Thermodynamics and Kinetics of Water–Rock Interaction. Rev. Mineral. 70, 207–258.
Soulsby, C., Malcolm, R., Helliwell, R., Ferrier, R.C., Jenkins, A., 2000. Isotope hydrology of the Allt a' Mharcaidh catchment, Cairngorms, Scotland: implications for hydrological pathways and residence times. Hydrol. Process. 14 (4), 747–762.
Stallard, R.F., Edmond, J.M., 1983. Geochemistry of the Amazon. 2. The influence of geology and weathering environment on the dissolved load. J. Geophys. Res. Oceans Atmos. 88 (NC14), 9671–9688.
Steefel, C.I., 2001. Software for Modeling Multicomponent, Multidimensional Reactive Transport*Rep*. UCRL-MA-143182, Lawrence Livermore National Laboratory, Livermore, CA.
Steefel, C.I., Lasaga, A.C., 1994. A coupled model for transport of multiple chemical species and kinetic precipitation dissolution reactions with application to reactive flow in single-phase hydrothermal systems. Am. J. Sci. 294 (5), 529–592.
Steefel, C.I., Maher, K., 2009. Fluid–rock interaction: a reactive transport approach, in Thermodynamics and Kinetics of Water–Rock Interaction. Rev. Mineral. 70, 485–532.
Steefel, C.I., Van Cappellen, P., 1990. A new kinetic approach to modeling water–rock interaction — the role of nucleation, precursors, and Ostwald ripening. Geochim. Cosmochim. Acta 54 (10), 2657–2677.
Stefansson, A., Gislason, S.R., 2001. Chemical weathering of basalts, Southwest Iceland: effect of rock crystallinity and secondary minerals on chemical fluxes to the ocean. Am. J. Sci. 301 (6), 513–556.
Stewart, M.K., Morgenstern, U., McDonnell, J.J., 2010. Truncation of stream residence time: how the use of stable isotopes has skewed our concept of streamwater age and origin. Hydrol. Process. 24 (12), 1646–1659.
Tardy, Y., 1971. Characterization of principal weathering types by geochemistry of waters from some European and African crystalline massifs. Chem. Geol. 7 (4), 253–271.
Tetzlaff, D., Seibert, J., McGuire, K.J., Laudon, H., Burn, D.A., Dunn, S.M., Soulsby, C., 2009. How does landscape structure influence catchment transit time across different geomorphic provinces? Hydrol. Process. 23 (6), 945–953.
Velbel, M.A., 1993. Temperature-dependence of silicate weathering in nature — how strong a negative feedback on long-term accumulation of atmospheric CO_2 and global greenhouse warming. Geology 21 (12), 1059–1062.
Violette, A., Godderis, Y., Marechal, J.C., Riotte, J., Oliva, P., Kumar, M.S.M., Sekhar, M., Braun, J.J., 2010. Modelling the chemical weathering fluxes at the watershed scale in the Tropics (Mule Hole, South India): relative contribution of the smectite/kaolinite assemblage versus primary minerals. Chem. Geol. 277 (1–2), 42–60.
Waldbauer, J.R., Chamberlain, C.P., 2005. Influence of uplift, weathering and base cation supply on past and future CO_2 levels. In: Ehleringer, et al. (Ed.), A History of Atmospheric CO_2 and Its Effects on Plants, Animals and Ecosystems. : Ecological Studies, 177. Springer Verlag, pp. 166–184.
Wallmann, K., 2001. Controls on the Cretaceous and Cenozoic evolution of seawater composition, atmospheric CO_2 and climate. Geochim. Cosmochim. Acta 65 (18), 3005–3025.
West, A.J., Bickle, M.J., Collins, R., Brasington, J., 2002. Small-catchment perspective on Himalayan weathering fluxes. Geology 30 (4), 355–358.
West, A.J., Galy, A., Bickle, M., 2005. Tectonic and climatic controls on silicate weathering. Earth Planet. Sci. Lett. 235 (1–2), 211–228.
White, A.F., Blum, A.E., 1995. Effects of climate on chemical weathering in watersheds. Geochim. Cosmochim. Acta 59 (9), 1729–1747.
White, A.F., Brantley, S.L., 2003. The effect of time on the weathering of silicate minerals: why do weathering rates differ in the laboratory and field? Chem. Geol. 202 (3–4), 479–506.
White, A.F., Schulz, M.S., Stonestrom, D.A., Vivit, D.V., Fitzpatrick, J., Bullen, T., Maher, K., Blum, A.E., 2009. Chemical weathering of a marine terrace chronosequence, Santa Cruz, California II: controls on solute fluxes and comparisons of long-term and contemporary mineral weathering rates. Geochim. Cosmochim. Acta 73, 2769–2803.
Wolery, T.J., Jackson, K.J., Bourcier, W.L., Bruton, C.J., Viani, B.E., Knauss, K.G., Delany, J. M., 1990. Current status of the EQ3/6 software package for geochemical modeling. ACS Symp. Ser. 416, 104–116.
Wolock, D.M., Fan, J., Lawrence, G.B., 1997. Effects of basin size on low-flow stream chemistry and subsurface contact time in the Neversink River Watershed, New York. Hydrol. Process. 11 (9), 1273–1286.
Yang, L., Steefel, C.I., 2008. Kaolinite dissolution and precipitation kinetics at 22 degrees C and pH 4. Geochim. Cosmochim. Acta 72 (1), 99–116.
Yurtsever, Y., 1999. Use of environmental tritium to study catchment dynamics: case study from the Danube River basin, in *Integrated Methods in Catchment Hydrology — Tracer, Remote Sensing and New Hydrometric Techniques*. Proceedings of an International Symposium held during IUGG 99, the XXII General Assembly of the International Union of Geodesy and Geophysics, at Birmingham, UK, 18–30. 167–176 pp.
Zeman, L.J., 1978. Mass balance model for calculation of ionic input loads in atmospheric fallout and discharge from a mountainous basin. Hydrol. Sci. Bull. 23, 103–117.
Zhu, C., Lu, P., Zheng, Z.P., Ganor, J., 2010. Coupled alkali feldspar dissolution and secondary mineral precipitation in batch systems: 4. Numerical modeling of kinetic reaction paths. Geochim. Cosmochim. Acta 74 (14), 3963–3983.